Published in final edited form as:
Biofabrication. 2014 June ; 6(2): 024113. doi:10.1088/1758-5082/6/2/024113.

Bioreactor for modulation of cardiac microtissue phenotype by combined static stretch and electrical stimulation

Jason W Miklas[1], **Sara S Nunes**[2], **Aarash Sofla**[1], **Lewis A Reis**[1], **Aric Pahnke**[1,4], **Yun Xiao**[1,4], **Carol Laschinger**, and **Milica Radisic**[1,2,3,4,*]

[1]Institute of Biomaterials and Biomedical Engineering, University of Toronto, Toronto, Ontario, Canada

[2]Toronto General Research Institute, University Health Network, Toronto, Ontario, Canada

[3]The Heart and Stroke/Richard Lewar Centre of Excellence, Toronto, Ontario, Canada

[4]Department of Chemical Engineering and Applied Chemistry, University of Toronto, Toronto, Ontario, Canada

Abstract

We describe here a bioreactor capable of simultaneously applying mechanical and electrical field stimulation in conjunction with static strain and on-line force of contraction measurements. It consisted of a polydimethylsiloxane (PDMS) tissue chamber and a pneumatically driven stretch platform. The chamber contained eight tissue microwells (8.05 mm in length and 2.5 mm in width) with a pair of posts (2.78 mm in height and 0.8 mm in diameter) in each well to serve as fixation points and for measurements of contraction force. Carbon rods, stimulating electrodes, were placed into the PDMS chamber such that one pair stimulated four microwells. For feasibility studies, neonatal rat cardiomyocytes were seeded in collagen gels into the microwells. Following three days of gel compaction, electrical field stimulation at 3–4 V/cm and 1Hz, mechanical stimulation of 5% static strain or electromechanical stimulation (field stimulation at 3–4 V/cm, 1Hz and 5% static strain) were applied for 3 days. Cardiac microtissues subjected to electromechanical stimulation exhibited elevated amplitude of contraction and improved sarcomere structure as evidenced by sarcomeric α-actinin, actin and troponin T staining compared to microtissues subjected to electrical or mechanical stimulation alone or non-stimulated controls. The expression of atrial natriuretic factor and brain natriuretic peptide was also elevated in the electromechanically stimulated group.

1 Introduction

Recent advances in the fields of stem cell biology [1–3] and cardiac tissue engineering [4–6] enable us to create human cardiac tissues *in vitro* [7, 8]. These tissues can potentially be used as platforms for drug testing or studies of cardiac physiology and pathophysiology. However, to enable correct utilization of these tissues in discovery studies, we need to find a way to mature cardiac tissues *in vitro*, induce desired disease phenotypes and enable on-line

*Correspondence to: M. Radisic, Institute of Biomaterials and Biomedical Engineering, University of Toronto, 164 College St, Toronto, ON, Canada M5S 3G9, m.radisic@utoronto.ca.

monitoring and recording of functional outputs such as force of contraction. Additionally, the resulting tissues should be composed of relatively small numbers of cells to reduce costs associated with high-throughput screening using cardiomyocytes derived from human pluripotent stem cells.

We have recently described a new platform for the generation of mature cardiac tissues termed biological wire or biowire [5]. The starting cell population were cardiomyocytes derived from either human embryonic stem cells or human induced pluripotent stem cells. The combination of three-dimensional cultivation in a micro-well and gel compaction around a suture enabled the creation of cardiac organoids with remarkably well developed structural properties with cells aligned in parallel with one another containing pronounced registers of sarcomeres. In addition, application of electrical field stimulation with a progressive frequency increase over 7 days of culture induced electrophysiological changes consistent with cell maturation including up regulation of I_{K1} and hERG currents. However, terminal differentiation was not achieved as demonstrated by the absence of T-tubules and M-lines at the ultrastructural level.

These findings motivated us to explore additional options that could result in terminal cell differentiation. Following biomimetic principles, we aimed to recreate the environment of the native heart tissue in a bioreactor in order to enable the cells to acquire and maintain a differentiated adult-like phenotype. One of the stimuli that was most strikingly lacking in our previous work was mechanical stimulation. In previous studies, mechanical stimulation led to physiological hypertrophy but induced elongation of action potential duration and did not seem to mature the calcium handling of the cardiomyocytes [9]. Interestingly, electrical stimulation improved cardiomyocyte calcium handling and also elicited a physiological hypertrophic response, albeit at incomplete levels [5]. Mechanical stretch has been shown to induce an active force-length relationship [4], similar to Frank-Starling curves generated from intact hearts, which was not present in cardiomyocytes derived from human pluripotent stem cells (hPSC) that were not subjected to mechanical stimulation [10]. Additionally, as the levels of load per cardiomyocyte are increased in the heart due to cell death in disease states such as in hypertension, pathological phenotypes of cardiomyocytes are induced and acquired. Therefore, we hypothesized that developing a platform which combined electrical and mechanical stimulation of cardiac microtissues would enable us to modulate the cardiomyocyte microenvironment to promote different levels of maturation or pathological conditions *in vitro*.

Currently, there are a variety of costly and time-consuming assays that can be employed to determine the phenotype of cardiomyocytes and function of the cardiac tissue as a whole. These include, confocal microscopy, transmission electron microscopy (TEM), real time quantitative polymerase chain reaction (RT-qPCR), immunohistochemistry, calcium transients mapping, optical mapping and patch clamping. In order to obtain a complete picture of the state of an individual cardiomyocyte in the tissue, all of these assays are required. However, besides being time-consuming, some of these assays (e.g. calcium transient recording and patch clamping) require the tissue to be digested at the end time point with plating of cells overnight which can possibly introduce errors. As a result, a quick method that uses the bulk tissue to determine changes consistent with maturation of

hypertrophy is needed. To address this, the platform developed here included a method to measure functional properties, specifically through the presence of posts that can deflect under the contractile force of the tissue as described in previous studies [9, 11–13]. Using two dimensional analytical solutions for a bending cantilever, the force of contraction of the tissue can be calculated from images acquired using bright filed microscopy and a camera. Additionally, the ability to acquire the force on-line can provide an effective way for screening different electromechanical regiments. Moreover, for the cardiac microtissue to beat as a whole and to beat faster in response to faster pacing the tissue must have functioning excitation-contraction coupling machinery. Consequently, if one assumes that as contractile force increases so does the maturation state of the cardiac microtissue then, screening for the force of contraction increase will also mean screening for the conditions that bring about the highest degree of maturation in the tissue. However, it should be noted that there are instances where high force can be associated with an immature, disease phenotype as found in pathological cardiac hypertrophy.

We describe here a bioreactor that enables con-current application of electrical and mechanical stimuli. Specifically, electrical field stimulation was combined with static strain. Cardiac microtissues were created by seeding cardiomyocytes in a well created from polydimethylsiloxane (PDMS), using a CNC (computer numerically controlled) machined mould, followed by gel compaction around two built-in posts. After 3 days of gel compaction a regiment of mechanical and/or electrical stimulation was applied for an additional 3 days. This initial study was focused on designing and proving feasibility of the bioreactor's use, thus all experiments were performed with cells derived from neonatal rat hearts. Future studies will focus on the use of hPSC-derived cardiomyocytes.

2 Methods

2.1 Neonatal rat heart isolation

Neonatal (1 to 2 day-old) Sprague-Dawley rats were euthanized according to the procedure approved by the University of Toronto Committee on Animal Care. The hearts were removed, quartered and the cells were isolated by an overnight treatment with trypsin (4°C, 6120 units/mL in Hank's Balanced Salt Solution, HBSS) followed by serial collagenase digestion (220 units/mL in HBSS) as described in previous work [14]. The supernatant from 5 collagenase digests of the tissues was collected and centrifuged at 750 RPM (94 × g) for 4 minutes, resuspended in culture medium and pre-plated into T75 flasks (Falcon) for two 1 hour intervals to separate the non-adherent cells (enriched cardiomyocytes) from the adherent cells (non-myocytes). The cells were cultivated in culture medium consisting of Dulbecco's Modified Eagle Medium (DMEM) with 4.5 g/L glucose, 4 mM L-glutamine, 10% certified fetal bovine serum (FBS), 100 U/mL penicillin, 100 μg/mL streptomycin, and 10 mM 4-2-hydroxyethyl-1-piperazineethanesulfonic acid buffer (HEPES, Gibco/Invitrogen).

2.2 Bioreactor platform design and manufacture

The bioreactor consisted of a PDMS tissue chamber capable of housing 8 microtissues, each in its own well and 2 pairs of stimulating electrodes. Four microtissues were stimulated by a

pair of the stimulating electrodes. The PDMS tissue chamber was then placed within a custom built stretch platform. To fabricate the PDMS tissue chamber, a 3D computer generated drawing of the mould was created using AutoCad, Figure 1A, B. Each microtissue well had a pair of posts to serve as fixation points for the tissue and for measurements of contraction force. The posts were designed to have a high aspect ratio of 3.5, where the height of each post was 2.78 mm and the diameter of each post was 0.8 mm. The distance between the centers of the two posts was set at 6.80 mm. This value was chosen so that the length of a cardiac microtissue would be about 7 mm. The AutoCad drawing was loaded into a milling machine that created a negative mould of the PDMS tissue chamber out of aluminum Figure 1C. To create the final device, the aluminum negative mould was filled with PDMS and allowed to cure at 80°C for 2hr at which point the PDMS tissue chamber was removed from the aluminum mould Figure 1D.

To provide mechanical stimulation, the PDMS tissue chamber was inserted into a pneumatically driven stretch device as shown in Figure 1E. The ends of the PDMS platform were sandwiched between two metal plates that served to anchor the PDMS tissue chamber platform to the stretch device. Compressed air was pumped into the pneumatic pistons to move the two plates of the stretch device apart stretching the entire PDMS platform. Finally, 3 mm (0.12 inch) diameter carbon rods (Ladd Research Industries) were inserted into the mould to provide the electrical field stimulation and connected to a commercially available Grass s88× stimulator as in our previous studies [5]. The displacement of the posts upon application of different levels of strain by the stretch platform was measured from microscopically acquired images using ImageJ to validate the bioreactor operating parameters.

2.3 Cell seeding

Cardiac microtissues were generated using enriched cardiomyocytes derived from neonatal rat hearts as described above. Sixty million cells/mL were suspended in 3.0 mg/mL collagen type I gels [15–17] (BD Biosciences) with 2 mM NaOH, 2.62 mM $NaHCO_3$, in 1X M199 media with 15% of the collagen gel solution consisting of growth factor reduced Matrigel (BD Biosciences). Twenty five μL of the cell gel suspension ($1.5 \cdot 10^6$ cells) was pipetted into each of the PDMS microtissue wells and placed into the incubator at 37°C for 30 minutes to allow the collagen hydrogel to gel. Microtissues were then cultured for three days with culture media changes every other day. Culture medium was the same as used in neonatal rat heart isolation. Subsequent, mechanical stimulation, electrical stimulation or a combination of electrical and mechanical stimulation was applied for three additional days. The electrical stimulation group had a pair of carbon electrodes placed in the PDMS tissue chamber at a distance of 2 cm from one another. The carbon electrodes were connected to a cardiac stimulator (Grass s88×) with platinum wires (Ladd Research Industries). Cardiac microtissues were situated perpendicular to the electrodes and were submitted to electrical stimulation (rectangular, biphasic, 1 ms, 3–4 V/cm) at 1Hz for three days. These electrical field stimulation parameters have been shown previously to work well in maturing rat neonatal cardiomyocyte patches [18]. For the group where mechanical and electrical stimulation was combined, the same electrical stimulation regiment as described above was used. In addition, to apply mechanical stimulation, the PDMS tissue chamber was placed

inside a custom made stretch platform Figure 1E. The PDMS tissue chamber was clamped into the metal base and by using compressed air to move a pair of pistons the PDMS tissue platform was stretched by 5%. This 5% stretch was transferred to the cardiac microtissues as they were anchored to two posts in each well. The 5% stretch was held constant for the duration of the three days of culture.

2.4 Post deflection measurements

To determine the force of contraction of each EHT, a cantilever beam-partial uniform load equation was used. At the end of cultivation, the PDMS tissue chamber was transferred into a controlled environment, at 37°C and 5% CO_2, microscope. To determine the force of contraction of each cardiac microtissue, the top surface of a post for one microtissue at a time was video recorded using CellSens software (Olympus). Post deflection for each microtissue was determined at increasing rates of stimulation frequency, starting at 0.5Hz and increasing to 3Hz at 0.5Hz increments. Each tracking video was taken for 30 seconds with 5 seconds in between starting a new tracking video at a higher frequency of pacing the microtissues. Each video was then exported as a series of Tiff images and opened in ImageJ. Using the ImageJ plugin SpotTracker [19], the distance the post moved was determined. Multiple measurements were used and then averaged to determine the average maximum post deflection, δ_{max}, for each cardiac microtissue at each frequency of pacing. The elastic modulus of the PDMS was determined prior the post-deflection measurements and an average obtained. The height of the post and the height of the tissue on the post were individually measured for each construct to ensure a precise calculation for each cardiac microtissue could be determined.

Since the EHTs were not situated at the bottom of the post, the method of superposition was implemented to determine the distributed load on the cantilever beam Figure 2B. To determine a partial uniform load at a specific distance along the beam's length, the subtraction of two different partial uniform distributed loads that all originate at the fixed end are used to determine the "floating" distributed load. The formula governing the method of superposition for a cantilever beam-partial uniform deflection is shown in [20], schematic of the cantilever beam is shown in Figure 2B, and variables for Equation 1 are defined in Table 1.

$$\delta_{max}=\frac{qa^3}{24EI}(4L-a)-\frac{qa'^3}{24EI}(4L-a') \quad \text{Eq. (1)}$$

In this case a = 2L/3 and a'=L/3 [20]

To determine the force per cross sectional area of each cardiac microtissue, the force per length q, was converted into a point load and divided by the cross sectional area of the cardiac microtissue. Each cross sectional area of the cardiac microtissue was individually measured using microscopy in conjunction with ImageJ. Four points along the length of the cardiac microtissue were measured and averaged to obtain the diameter of the cardiac microtissue, assuming circular cross section, to determine each specific cardiac microtissue cross-sectional area. Equation 2 was used to calculate force per unit area.

$$FPA = \frac{qa}{\pi r^2} \quad \text{Eq. (2)}$$

Sensitivity analysis was performed to determine at which magnitudes different factors influence the calculated force per area measurements.

2.5 Validation of the force of contraction measurements

Validation of the calculated force required to move the PDMS post was performed using direct measurements on the Refined Myograph System (Kent Scientific). The PDMS post and part of the base was excised from the PDMS platform and placed on a glass slide. Since the Myograph has a caliper attached to the force transducer, specific displacements were measured while recording a change in voltage from the transducer, which correlated to the force needed to displace the tip of a single PDMS post. A displacement versus force graph was then generated.

2.6 Measurements of elastic modulus of the PDMS

To determine the elastic modulus of the PDMS, a rectangular strip of PDMS was created for tensile testing. Using an ElectroForce 5200 BioDynamic Test Instrument (Bose) tensile testing machine, a constant rate of displacement (1 mm/min) and stretch distance was set. The software, WinTest, was used to collect the displacement and the force generated. Finally, the stress was calculated and a stress strain curve was generated where the slope of the data set represented the elastic modulus. The curves were linear over the entire range tested ($R^2 = 0.99$), up to 35% strain, thus at the given composition our PDMS behaved as a linear elastic material.

2.7 Excitation threshold and maximum capture rate measurements

After six days of culture, cardiac microtissues were assessed for two functional parameters: excitation threshold (ET) and maximum capture rate (MCR). ET and MCR were measurements performed in a controlled environment of 37°C and 5% CO_2. ET was determined as the lowest voltage the cardiac microtissues could be continuously paced at 2 Hz. MCR was determined as the highest frequency of continuous pacing the microtissues could exhibit at 5–6 V/cm.

2.8 Confocal microscopy

At the final time point of six days, cardiac microtissues were fixed in 4% paraformaldehyde. Immunostaining was performed as described previously [5] using the following antibodies: mouse anti-cardiac troponin T (cTNT) (Abcam; 1:100), mouse anti-α-actinin (Abcam, 1:20), rabbit anti-connexin 43 (Cx43) (Abcam, 1:500), goat anti-mouse-Alexa Fluor 488 (Jackson ImmunoResearch; 1:400) and donkey anti-rabbit-TRITC (Invitrogen; 1:400). Phalloidin (Invitrogen 1:100) was used to detect actin fibers. Cells were visualized using a fluorescence confocal microscope (Zeiss LSM-510).

2.9 Quantitative polymerase chain reaction (qPCR)

Real time qPCR was performed as previously described [5]. Total RNA was prepared from cardiac microtissues after six days of culture following the manufacturer's protocol for TRIzol Reagent (Invitrogen). RNA was reverse transcribed into cDNA using random hexamers and Oligo (dT) with SuperScript VILO (Invitrogen). RT-qPCR was performed on a LightCycler 480 (Roche) using LightCycler 480 SYBR Green I Master (Roche). Expression levels were normalized to the housekeeping gene Glyceraldehyde 3-phosphate dehydrogenase (GAPDH). The oligonucleotide sequences are summarized in Supplemental Table 1.

2.10 Western blotting

Cardiac microtissue protein was isolated after six days of culture following the manufacturer's protocol for TRIzol Reagent (Invitrogen). Once the protein was isolated, the protein pellet was solubilized in a 1% SDS solution in de-ionized water. Proteins were separated by electrophoresis in Novex Tris-Glycine gels (Life technologies) and dry transferred using the iBlot (Life technologies) to a nitrocellulose iBlot Transfer Stack (Life technologies). Membranes were probed for Phospho-p44/42 MAPK (pERK1/2) (Cell Signaling Technology), p44/42 MAPK (ERK1/2) (Cell Signaling Technology), or GAPDH (Millipore) antibodies. Secondary antibodies were peroxidase conjugated (DAKO). Membranes were developed with ECL reagent LuminataClassico Substrate (Millipore).

2.11 Statistical Analysis

Statistical analysis was performed using SigmaPlot 12.0. Differences between experimental groups were analyzed by One or Two-Way ANOVA. For One-Way ANOVA, Kolmogorov-Smirnov was used for the normality test. For a failed normality test during One-Way ANOVA, Kruskal-Wallis One-Way ANOVA on Ranks was used. For Two-Way ANOVA, the Shapiro-Wilk normality test and Holm-Sidak method for pairwise multiple comparison procedures were used. $P < 0.05$ was considered significant for all statistical tests.

3 Results

3.1 Validation of the bioreactor platform operation

In order to have a uniform and controllable amount of static stress applied to the cardiac microtissues, we needed to ensure that the strain distribution within the PDMS microtissue wells was uniform and equal in all the microtissue wells. Additionally, we needed to ensure that as the PDMS well was stretched using the bioreactor platform, the distance between the two posts in the cardiac microtissues increased equally in different microtissue wells, and proportionally to the amount of strain applied to the entire PDMS platform. This validation was achieved by direct measurements from microscopically acquired images.

As seen in Table 2, the actual displacement of the posts was shown as a percent change in the distance. For the 5% and 10% strain applied to the PDMS well by the bioreactor platform, the achieved displacement between the anchoring posts was 4.6% and 10.5%, resulting in a relatively small error. As the applied strain increased to 15% and 20%, the actual displacement between the posts began to falter to 13.3% and 16.9% resulting in

unacceptably large percent error for the highest strain applied. Thus, we concluded that the developed platform should be used in conjunction with strains of up to 15%.

It was also necessary for us to confirm that the forces of contraction calculated using the analytical solution of the beam-deflection model was correct. This was achieved by measuring, using an independent instrument, the amount of force needed to bend the PDMS post by a certain amount. Percent error in evaluation was then calculated based upon the difference between the Myograph testing and the analytical solution as seen in Table 3 with an average percent error of 7.4±4.1%.

Finally, a sensitivity analysis was performed to determine the relationship between tissue height and deflection of the post at the free end and to also examine the relationship between a tissue's force of contraction and the deflection of the post at the free end. Figure 2C shows how the deflection of the post at the free end changes based on how the height of the tissue varies from the bottom of the post to the top of the post. In this scenario it is assumed that the tissue thickness was 0.4 mm and the percentage change in height was the difference between the tissue's new height along the post and the ideal position of the tissue, which is when the tissue is sitting at the bottom of the post. Clearly, the force of contraction calculation is very sensitive to the position of the tissue along the post as the post deflects much easier under the same load as the tissue is positioned at higher positions (moving away from the base and towards the tip of the post). Consequently, it is important to determine the tissue's position along the post each time post deflection imaging is performed by determining the Z-displacement from the top of the post to the tissue. On average, the height of the tissues measured were 1.72±0.36 mm above the base of the post when force of contraction was assessed on day 7. This corresponds to a percent change in height from the base of the post of 330% when referring to Figure 2C. For the post to be deflected 1 μm at this height, assuming an average tissue thickness of 0.4 mm (as in Figure 2C and D), the average distributed load would need to be 0.02 N/m which corresponds to a point load of 0.008 mN or 0.064 mN/mm^2. The smallest stress that we measured in our system was 0.093 mN/mm^2. Furthermore, each tissue's width needs to be measured to determine the cross sectional area to calculate force per area as shown in Figure 2A.

Figure 2D shows how the force of contraction of a cardiac microtissue, or the distributed load along the post, affects the maximum deflection at the free end. In this scenario, the original distributed load was set to be 0.5 N/m, which is a point-load of 0.2 mN. At 0.2 mN the free end will deflect about 1 μm, which is the lower limit of the displacement that could be measured using this set-up due to the optical transparency limitations of the PDMS and the tissue.

3.2 Cardiac microtissues generated in the bioreactor platform

Our main goal here was to determine if the newly developed bioreactor platform could support survival of cardiomyocytes and their assembly into contractile tissue, as well as to determine if the differences between electrical field stimulation alone compared to the combined electromechanical stimulation regimen could be detected. We therefore used cardiomyocytes derived from neonatal rat hearts to generate cardiac microtissues in non-stimulated, non-stretched controls; electrical field stimulation alone or in the presence of

both electrical field stimulation and static stretch. To allow cells to elongate and remodel the matrix first, stimulation regimens were initiated after 3 days of stimulation-free pre-culture. Initiating stimulation too early was found detrimental in our previous work [18] and would likely lead to rupture of the tissue here. At the end of culture, there were no significant differences in electrical excitability parameters, excitation threshold and maximum capture rate, between the three groups (Figure 3A, B). However, force of contraction was increased in the group that was subject to con-current electromechanical stimulation and found to be statistically significant at 0.5Hz (P=0.003), 1.0Hz (P=0.004), 1.5Hz (P=0.006), 2.0Hz (p=0.0017) and 2.5Hz (P=0.028) in comparison to the 5% strain group (Figure 3C). Representative traces of each condition being paced at frequencies between 0.5–3Hz are shown in Supplemental Figure 1.

Immunostaining demonstrated that cardiac microtissues subjected to concurrent electromechanical stimulation exhibited well developed sarcomeric structures in comparison to those subjected to electrical field stimulation alone, mechanical strain alone or to the control cardiac microtissues. Double staining for sarcomeric α-actinin and actin revealed well developed registers of sarcomeres in the 5% strain + 1Hz group, whereas this organization was not as apparent in the other three groups (Figure 4A). Furthermore, the 5% strain group displayed poor myofibril formation with some myofibrils aligning perpendicular to the static strain direction in comparison to previous cardiac tissue engineered studies showing cyclic stretching (10%, 2Hz) [21] or auxotonic loads [22] (Supplemental Figure 2). This poor response is typically found in 2D static and cyclic strain cultures as cardiomyocytes rearrange themselves to elongate in a transverse direction to the strain, i.e. to experience less strain [23, 24]. This result may also account for the lower force produced by the 5% strain condition. Double staining for cardiac troponin T and connexin-43, revealed well defined cross striation of cTnT in the 5% strain + 1Hz group. The gap-junctional protein, connexion-43, was present in all conditions (Figure 4B).

Sarcomeric proteins α-myosin heavy chain (MHC) and β-myosin heavy chain are differentially regulated in mammalian hearts during development. In rodents, α-MHC is upregulated compared to β-MHC during maturation while, the opposite holds true for humans [12]. Quantitative PCR demonstrated similar α-MHC/β-MHC ratios in all four conditions with the 5% strain group being the lowest, which indicated that at the current conditions, no appreciable shift towards maturation was occurring over 6 days of total culture of neonatal rat cardiac microtissues (Figure 5A). The lower average α/βMHC ratio in the 5% strain group may point towards a pathological state [25]. Sarco/endoplasmic reticulum Ca^{2+} ATP-ase (SERCA) is an ion pump found in the membrane of the sarcoplasmic reticulum that is responsible for pumping Ca^{2+} back from the cytoplasm into the sarcoplasmic reticulum at the completion of a contraction cycle in mature cardiomyocytes [10, 26]. There were no significant differences in SERCA expression amongst the three groups (Figure 5B) in cardiac microtissues. Atrial natriuretic factor (ANF) and brain natriuretic peptide (BNP) are molecules highly expressed in ventricular cardiomyocytes in the late stages of rodent and human heart development [27]. In the post-natal and adult stages, the re-expression of these proteins is consistent with pathological hypertrophy [28]. The fact that ANF was highly expressed in the 5% strain + 1Hz and BNP was highly expressed in the 5% strain and 5% strain + 1Hz groups might indicate that these

cells were at the on-set of the pathological hypertrophy process (Figure 5C, D) however no clear signs of sarcomere destruction were observed in the immunostaining samples. To gauge the levels of cell apoptosis vs. survival in different groups we examined the expression levels of mRNAs for proteins in the B-cell lymphoma family (Bcl) [12]. There were no significant differences in the ratio of pro-apoptotic Bax to anti-apoptotic Bcl-2 in the four groups, indicating that electrical field stimulation, mechanical stimulation, concurrent electromechanical stimulation and the control non-stimulated condition were all equally conducive to survival of the cells in PDMS wells.

To further investigate the induction of a hypertrophic response with stimulation in the bioreactor platform we investigated the levels of ERK1/2 and phosphorylation levels of ERK1/2 as phospho ERK1/2 has been previously shown to be associated with physiological hypertrophy [29]. As shown in Figure 6, total levels of ERK1/2 were comparable amongst the three groups and the levels of phospho ERK1/2 were slightly although not significantly elevated in either 1Hz, 5% strain or the 5% strain + 1Hz condition compared to the control condition. The ratio of phospho ERK/ERK was comparable in all conditions except 5%, which was statistically significant in comparison to control (P=0.032).

4 Discussion

Native heart muscle consists of aligned cardiomyocytes that contract synchronously as a result of rapid action potential propagation between adjacent cardiomyocytes via gap junctions. This coordinated action of cardiomyocytes results in pumping and expulsion of blood from the ventricles. As the ventricles relax, they are filled with blood causing the ventricular volume to expand and the ventricular wall to stretch. Thus, at each contraction cycle *in vivo*, cardiomyocytes contract against the load (i.e. blood filling the ventricles) and the electrical stimulus arises when the ventricular wall is in the stretched state. Ventricular cardiomyocytes have a number of stretch activated ion channels that are important regulators of cardiomyocyte functionality [30]. The importance of physical stretch was realised in the earliest cardiac tissue engineering studies [12, 21, 31–33] and early cardiac tissues based on neonatal rat cardiomyocytes cultivated in the presence of cyclic mechanical stretch. Zimmermann and Eschenhagen demonstrated that when neonatal rat cardiomyocytes were stimulated at 10% stretch and a frequency of 2Hz, they could be pushed to a mature phenotype similar to the one found in the native adult heart as evidenced by the presence of Z, I, A and H bands in the sarcomeres as well as T-tubules [31]. Additionally, cyclic stretching led to physiological hypertrophy as evidenced by increased cardiomyocytes size, increased percentage of binucleated cardiomyocytes and upregulation of the ventricular isoform of myosin light chain [12]. Engineered cardiac tissues that were cultivated under auxotonic load were implanted in a rat model of myocardial infarction mitigating heart failure [22]. This study also conclusively demonstrated integration of rat engineered heart tissues with the native rat myocardium [22].

Mechanical loading was also used to stimulate cardiomyocytes derived from human pluripotent stem cells. Since cyclic stretch was able to mature neonatal rat cardiomyocytes to an adult like stage, Tulloch *et al.* [4] implemented a similar set-up using cyclic stretch to try and mature hPSC-derived cardiomyocytes. Similarly, cyclic stretch promoted a pro-

hypertrophic response in these cells as illustrated by increased cell alignment parallel to the mechanical loading force, increased DNA synthesis, increased cardiomyocyte area, and induction of βMHC, cTnT, L-type calcium channel, ryanodine receptor, and SERCA mRNA compared to the constructs that were cultivated in the absence of loading [4].

Interestingly, Kensah *et al.* [34] found that cyclic stretch (10%; 1Hz for 7 days) did not improve contractile function or morphology of their cardiac tissue engineered constructs in comparison to static stretch. Instead of cyclic stretch, they generated a protocol that gradually increased the static strain of their constructs over 14 days with increases in static strain occurring every second day in an attempt to recapitulate the increasing systolic and diastolic pressure in the developing heart. Similar to our findings, they did not see a statistically significant increase in maximum active force of their gradually increasing static strain group in comparison to their control. They did not see an increase in BNP or ANF gene expressing in their gradually increasing static strain group [34]. Yet, in their gradually increasing static strain group they did have aligned sarcomeres parallel to the stretching force while, we found that our large single increase in static stress resulted in cardiomyocytes elongating perpendicular to the stretching direction, most likely in an attempt to reduce the strain on their system. This could also account for the decreased force of contraction that was observed, albeit not statistically significant to control.

While these results with cyclic stretch alone were encouraging, there was scarce evidence that mechanical stimulation alone was sufficient to mature certain aspects of the calcium handling machinery and induce appropriate expression and function of diverse ion channels required for cardiac function. Engineered heart tissues generated from hPSC derived cardiomyocytes displayed abnormally long action potential durations (up to 1200ms) and a resting membrane potential of −49.1 mV [9] which, is less negative than the resting membrane potential of comparable 7–8 week old embryoid bodies that resulted in cardiomyocytes with resting membrane potential of −60.7 mV.

Interestingly, mechanical stimulation could also be provided by a compressive fluid flow as we [35] and others [36] have demonstrated previously. When mechanical compression was provided together with fluid shear instead of stretching in a static vessel to stimulate neonatal rat cardiomyocytes, an intermittent compression regiment was able to preserve α-actinin and N-cadherin expression and improve Cx43 expression compared to non-compressed controls [36]. Fluid shear could also induce a physiological hypertrophic response, mediated through the ERK1/2 signaling pathway, as evidenced by upregulation of protein synthesis [29].

One of the other major parameters that has been shown to affect functionality of engineered heart tissues is cell alignment. Many cardiac tissue engineering studies relied upon gel compaction, of either fibrin or collagen gels, to generate engineered heart tissues with aligned cardiomyocytes. Passive tensile force was usually generated in these systems by two anchoring posts or using a cylindrical non-adhesive mold. Black *et al*. [37] systematically showed that engineered heart tissues which undergo gel compaction contain well aligned cells. This increased cell alignment in turn prompted an increased phosphorylated state of Cx43. Both of these factors resulted in higher forces of contraction in the aligned engineered

heart tissues in comparison to those that had randomly oriented cells [37]. This finding shows the importance of anisotropy in engineered myocardium and the importance of cardiomyocyte elongation with tension for proper maturation. Optimizing and enhancing mechanical stimulation platforms is an area of active research as evidenced by recent reports of novel bioreactors capable of mechanical stimulation [38, 39].

We first started using electrical field stimulation in cardiac tissue engineering using cardiomyocytes derived from neonatal rat hearts. The cells were seeded into porous collagen scaffold and subjected to field stimulation for 5 days after a pre-culture for 3 days allowed the cells to elongate in the matrix. Electrically stimulated samples were able to form well aligned registers of sarcomeres and exhibit defined M and Z lines and H, I, and A bands [18]. Recently, we used electrical stimulation of progressive frequency increase to mature cardiomyocytes derived from human pluripotent stem cells cultivated in microstructures termed biowire [5].

Our goal here was to develop a platform that can provide combined electromechanical stimulation and prove the feasibility of its operation. Electromechanical stimulation of scaffold-based engineered tissues have recently been reported by Wang *et al.* [40] and Morgan *et al*. [41]. However, the platform designed by Wang *et al*. was only validated using mesenchymal stem cells (MSCs) as the cell source and both aforementioned designs did not utilize on-line force readout. Liao *et al.* created an electromechanical stimulation platform that had online force of contraction measuring, however, only one cardiac construct could be created and measured per bioreactor. The platform described here provides a relatively high throughput system, 8 cardiac microtissues per PDMS platform, in comparison to other platforms that usually can only accommodate one or two constructs per platform [38, 39, 42]. While our platform is similar to *Boudou et al.* [13] they did not mechanically stretch their cardiac constructs to observe the effects of combined mechanical strain and electrical stimulation.

One of the main aims of this work was to demonstrate that cardiomyocytes can survive, function and form a contractile tissue in the developed bioreactor platform. We therefore focused on the use of readily available neonatal rat heart cells, while the use of cardiomyocytes derived from human pluripotent stem cells will be reserved for future studies. In future studies, electromechanical stimulation protocols will be optimized with these cells and the possible parameter space may include intermitted application of electrical stimulation on stretched samples, application of auxotonic or cyclic mechanical stimulation in conjunction with electrical stimulation as well as switching from field to point stimulation. We have previously extensively utilized electrical field stimulation in cardiac tissue engineering [5, 43], thus we wanted to evaluate here if the application of electromechanical stimulation will result in additional changes in the cardiac microtissues compared to the application electrical or mechanical stimulation alone.

The values of electrical excitability parameters obtained here (Figure 3A,B) were in the same range as those we previously reported [43], however the differences between the control and stimulated groups were not apparent, likely due to the short stimulation time (3 days) in comparison to longer stimulation times (5–21 days) we used in previous studies [5,

43, 44]. As expected, force of contraction increased with the presence of electromechanical stimulation (Figure 3C). While the force measurements we obtained were not as high as previously reported groups [45], when culture time is taken into consideration our force values (0.05–0.15mN at day 6) match well with previous reports of engineered heart tissue cultured for similar times (0.1mN at day 8) [9, 11, 46]. It is possible that after two weeks of culture the force generated by the cardiac micro tissues presented in this paper may match the force generated by *Hirt et al.* [11]. We did not observe a positive force-frequency relationship (Figure 3C). We are convinced that this is due to a short total cultivation time (6 days) and a short stimulation time (3 days). Previous mechanical stimulation studies have also been unable to observe a positive force frequency relationship due to increased pacing rate that is found in adult mouse ventricular cardiomyocytes [47], however, they do show a positive active force-length relationship during increasing strain (Frank-Starling mechanism) at time points of 9–10 days [31] and 14 days [21].

Further analysis is required to determine if the improved sarcomere structure observed in the 5% strain + 1Hz condition (Figure 4) is truly a result of physiological hypertrophy alone or if the pathological hypertrophy process is being initiated in this group based on the upregulation of ANF and BNP (Figure 5C,D). Since the onset of pathological hypertrophy takes longer than 3 days, future studies of longer stretch time periods will explore this disease state. Moreover, the increased ratio of pERK1/2 to ERK1/2 in the 5% strain group contrasted to the low force of contraction, possibly due to poor alignment of myofibrils, and high BNP expression requires further investigation (Figure 3 and 6). The developed bioreactor platform enables us to optimize the modalities of electromechanical stimulation to achieve either physiological or pathological hypertrophy for future studies. Importantly, none of the stimulation modalities applied here were detrimental in terms of enhancing cell apoptosis as evidenced by the unchanged ratio of Bax/Bcl2 in the three groups (Figure 5E). Overall, we described here a new bioreactor that can be used to study biological phenomena, such as cardiomyocyte hypertrophy, with further studies needed to delineate mechanistic effects of electro-mechanical stimulation.

5 Conclusion

We developed a bioreactor that enabled us to apply con-current electrical and static strain stimulation to cardiac microtissues. The operation of the bioreactor was validated by the cultivation of cardiac microtissues based on neonatal rat cardiomyocytes. The tissue compacted over 3 days of culture and an additional 3 days of stimulation resulted in the improved sarcomere structure and increased force in the group subjected to electromechanical stimulation. Future studies are required to optimize the bioreactor for either pathological or physiological hypertrophy in cardiomyocytes derived from human pluripotent stem cells.

Supplementary Material

Refer to Web version on PubMed Central for supplementary material.

Acknowledgments

The authors would like to thank the University of Toronto MIE Machine shop for their assistance in building the stretch platform. This work was funded by grants from Ontario Research Fund–Global Leadership Round 2 (ORF-GL2), National Sciences and Engineering Research Council of Canada (NSERC) Strategic Grant (STPGP 381002-09), Canadian Institutes of Health Research (CIHR) Operating Grant (MOP-126027), NSERC-CIHR Collaborative Health Research, Grant (CHRPJ 385981-10), NSERC Discovery Grant (RGPIN 326982-10) and NSERC Discovery Accelerator Supplement (RGPAS 396125-10).

References

1. Yang L, Soonpaa MH, Adler ED, Roepke TK, Kattman SJ, Kennedy M, Henckaerts E, Bonham K, Abbott GW, Linden RM, Field LJ, Keller GM. Human cardiovascular progenitor cells develop from a KDR+ embryonic-stem-cell-derived population. Nature. 2008; 453:524–528. [PubMed: 18432194]
2. Zhang J, Wilson GF, Soerens AG, Koonce CH, Yu J, Palecek SP, Thomson JA, Kamp TJ. Functional cardiomyocytes derived from human induced pluripotent stem cells. Circ Res. 2009; 104:e30–e41. [PubMed: 19213953]
3. Didie M, Christalla P, Rubart M, Muppala V, Doker S, Unsold B, El-Armouche A, Rau T, Eschenhagen T, Schwoerer AP, Ehmke H, Schumacher U, Fuchs S, Lange C, Becker A, Tao W, Scherschel JA, Soonpaa MH, Yang T, Lin Q, Zenke M, Han DW, Scholer HR, Rudolph C, Steinemann D, Schlegelberger B, Kattman S, Witty A, Keller G, Field LJ, Zimmermann WH. Parthenogenetic stem cells for tissue-engineered heart repair. J Clin Invest. 2013; 123:1285–1298. [PubMed: 23434590]
4. Tulloch NL, Muskheli V, Razumova MV, Korte FS, Regnier M, Hauch KD, Pabon L, Reinecke H, Murry CE. Growth of engineered human myocardium with mechanical loading and vascular coculture. Circ Res. 2011; 109:47–59. [PubMed: 21597009]
5. Nunes SS, Miklas JW, Liu J, Aschar-Sobbi R, Xiao Y, Zhang B, Jiang J, Masse S, Gagliardi M, Hsieh A, Thavandiran N, Laflamme MA, Nanthakumar K, Gross GJ, Backx PH, Keller G, Radisic M. Biowire: a platform for maturation of human pluripotent stem cell-derived cardiomyocytes. Nat Methods. 2013; 10:781–787. [PubMed: 23793239]
6. Caspi O, Lesman A, Basevitch Y, Gepstein A, Arbel G, Habib IH, Gepstein L, Levenberg S. Tissue engineering of vascularized cardiac muscle from human embryonic stem cells. Circ Res. 2007; 100:263–272. [PubMed: 17218605]
7. Chiu LL, Iyer RK, Reis LA, Nunes SS, Radisic M. Cardiac tissue engineering: current state and perspectives. Front Biosci (Landmark Ed). 2012; 17:1533–1550. [PubMed: 22201819]
8. Nunes SS, Song H, Chiang CK, Radisic M. Stem cell-based cardiac tissue engineering. J Cardiovasc Transl Res. 2011; 4:592–602. [PubMed: 21748529]
9. Schaaf S, Shibamiya A, Mewe M, Eder A, Stohr A, Hirt MN, Rau T, Zimmermann WH, Conradi L, Eschenhagen T, Hansen A. Human engineered heart tissue as a versatile tool in basic research and preclinical toxicology. PLoS One. 2011; 6:e26397. [PubMed: 22028871]
10. Binah O, Dolnikov K, Sadan O, Shilkrut M, Zeevi-Levin N, Amit M, Danon A, Itskovitz-Eldor J. Functional and developmental properties of human embryonic stem cells-derived cardiomyocytes. J Electrocardiol. 2007; 40:S192–S196. [PubMed: 17993321]
11. Hirt MN, Sorensen NA, Bartholdt LM, Boeddinghaus J, Schaaf S, Eder A, Vollert I, Stohr A, Schulze T, Witten A, Stoll M, Hansen A, Eschenhagen T. Increased afterload induces pathological cardiac hypertrophy: a new in vitro model. Basic Res Cardiol. 2012; 107:307. [PubMed: 23099820]
12. Tiburcy M, Didie M, Boy O, Christalla P, Doeker S, Naito H, Karikkineth BC, El-Armouche A, Grimm M, Nose M, Eschenhagen T, Zieseniss A, Katschinksi D, Hamdani N, Linke WA, Yin X, Mayr M, Zimmermann WH. Terminal Differentiation, Advanced Organotypic Maturation, and Modeling of Hypertrophic Growth in Engineered Heart Tissue. Circ Res. 2011
13. Boudou T, Legant WR, Mu A, Borochin MA, Thavandiran N, Radisic M, Zandstra PW, Epstein JA, Margulies KB, Chen CS. A Microfabricated Platform to Measure and Manipulate the Mechanics of Engineered Cardiac Microtissues. Tissue engineering. Part A. 2012

14. Radisic M, Park H, Shing H, Consi T, Schoen FJ, Langer R, Freed LE, Vunjak-Novakovic G. Functional assembly of engineered myocardium by electrical stimulation of cardiac myocytes cultured on scaffolds. Proc Natl Acad Sci U S A. 2004; 101:18129–18134. [PubMed: 15604141]
15. Nunes SS, Greer KA, Stiening CM, Chen HY, Kidd KR, Schwartz MA, Sullivan CJ, Rekapally H, Hoying JB. Implanted microvessels progress through distinct neovascularization phenotypes. Microvasc Res. 2010; 79:10–20. [PubMed: 19833141]
16. Nunes SS, Krishnan L, Gerard CS, Dale JR, Maddie MA, Benton RL, Hoying JB. Angiogenic potential of microvessel fragments is independent of the tissue of origin and can be influenced by the cellular composition of the implants. Microcirculation. 2010; 17:557–567. [PubMed: 21040121]
17. Nunes SS, Rekapally H, Chang CC, Hoying JB. Vessel arterial-venous plasticity in adult neovascularization. PLoS One. 2011; 6:e27332. [PubMed: 22132096]
18. Radisic M, Park H, Shing H, Consi T, Schoen FJ, Langer R, Freed LE, Vunjak-Novakovic G. Functional assembly of engineered myocardium by electrical stimulation of cardiac myocytes cultured on scaffolds. Proc Natl Acad Sci U S A. 2004; 101:18129–18134. [PubMed: 15604141]
19. Sage D, Neumann FR, Hediger F, Gasser SM, Unser M. Automatic tracking of individual fluorescence particles: Application to the study of chromosome dynamics. IEEE Transactions on Image Processing. 2005; 14:1372–1383. [PubMed: 16190472]
20. Gere JM, Goodno BJ. Mechanics of Materials, SI Edition, 8th ed.: Si Edition. 2012 Cengage Learning).
21. Zimmermann WH, Schneiderbanger K, Schubert P, Didie M, Munzel F, Heubach JF, Kostin S, Neuhuber WL, Eschenhagen T. Tissue engineering of a differentiated cardiac muscle construct. Circ Res. 2002; 90:223–230. [PubMed: 11834716]
22. Zimmermann WH, Melnychenko I, Wasmeier G, Didie M, Naito H, Nixdorff U, Hess A, Budinsky L, Brune K, Michaelis B, Dhein S, Schwoerer A, Ehmke H, Eschenhagen T. Engineered heart tissue grafts improve systolic and diastolic function in infarcted rat hearts. Nat Med. 2006; 12:452–458. [PubMed: 16582915]
23. Salameh A, Wustmann A, Karl S, Blanke K, Apel D, Rojas-Gomez D, Franke H, Mohr FW, Janousek J, Dhein S. Cyclic mechanical stretch induces cardiomyocyte orientation and polarization of the gap junction protein connexin43. Circ Res. 2010; 106:1592–1602. [PubMed: 20378856]
24. Matsuda T, Takahashi K, Nariai T, Ito T, Takatani T, Fujio Y, Azuma J. N-cadherin-mediated cell adhesion determines the plasticity for cell alignment in response to mechanical stretch in cultured cardiomyocytes. Biochem Biophys Res Commun. 2005; 326:228–232. [PubMed: 15567175]
25. Iemitsu M, Miyauchi T, Maeda S, Sakai S, Kobayashi T, Fujii N, Miyazaki H, Matsuda M, Yamaguchi I. Physiological and pathological cardiac hypertrophy induce different molecular phenotypes in the rat. Am J Physiol Regul Integr Comp Physiol. 2001; 281:R2029–R2036. [PubMed: 11705790]
26. Dolnikov K, Shilkrut M, Zeevi-Levin N, Gerecht-Nir S, Amit M, Danon A, Itskovitz-Eldor J, Binah O. Functional properties of human embryonic stem cell-derived cardiomyocytes: intracellular Ca2+ handling and the role of sarcoplasmic reticulum in the contraction. Stem Cells. 2006; 24:236–245. [PubMed: 16322641]
27. Razeghi P, Young ME, Alcorn JL, Moravec CS, Frazier OH, Taegtmeyer H. Metabolic gene expression in fetal and failing human heart. Circulation. 2001; 104:2923–2931. [PubMed: 11739307]
28. Kong SW, Bodyak N, Yue P, Liu Z, Brown J, Izumo S, Kang PM. Genetic expression profiles during physiological and pathological cardiac hypertrophy and heart failure in rats. Physiol Genomics. 2005; 21:34–42. [PubMed: 15623566]
29. Dvir T, Levy O, Shachar M, Granot Y, Cohen S. Activation of the ERK1/2 cascade via pulsatile interstitial fluid flow promotes cardiac tissue assembly. Tissue Eng. 2007; 13:2185–2193. [PubMed: 17518740]
30. Zipes, DP.; Jalife, J. Cardiac electrophysiology: from cell to bedside. Saunders/Elsevier; 2009.

31. Zimmermann WH, Fink C, Kralisch D, Remmers U, Weil J, Eschenhagen T. Three-dimensional engineered heart tissue from neonatal rat cardiac myocytes. Biotechnol Bioeng. 2000; 68:106–114. [PubMed: 10699878]
32. Akhyari P, Fedak PW, Weisel RD, Lee TY, Verma S, Mickle DA, Li RK. Mechanical stretch regimen enhances the formation of bioengineered autologous cardiac muscle grafts. Circulation. 2002; 106:I137–I142. [PubMed: 12354723]
33. Boublik J, Park H, Radisic M, Tognana E, Chen F, Pei M, Vunjak-Novakovic G, Freed LE. Mechanical properties and remodeling of hybrid cardiac constructs made from heart cells, fibrin, and biodegradable, elastomeric knitted fabric. Tissue Eng. 2005; 11:1122–1132. [PubMed: 16144448]
34. Kensah G, Roa Lara A, Dahlmann J, Zweigerdt R, Schwanke K, Hegermann J, Skvorc D, Gawol A, Azizian A, Wagner S, Maier LS, Krause A, Drager G, Ochs M, Haverich A, Gruh I, Martin U. Murine and human pluripotent stem cell-derived cardiac bodies form contractile myocardial tissue in vitro. Eur Heart J. 2013; 34:1134–1146. [PubMed: 23103664]
35. Brown MA, Iyer RK, Radisic M. Pulsatile perfusion bioreactor for cardiac tissue engineering. Biotechnol Prog. 2008; 24:907–920. [PubMed: 19194900]
36. Shachar M, Benishti N, Cohen S. Effects of mechanical stimulation induced by compression and medium perfusion on cardiac tissue engineering. Biotechnol Prog. 2012; 28:1551–1159. [PubMed: 22961835]
37. Black LD 3rd, Meyers JD, Weinbaum JS, Shvelidze YA, Tranquillo RT. Cell-induced alignment augments twitch force in fibrin gel-based engineered myocardium via gap junction modification. Tissue engineering. Part A. 2009; 15:3099–3108. [PubMed: 19338433]
38. Nguyen MD, Tinney JP, Yuan F, Roussel TJ, El-Baz A, Giridharan G, Keller BB, Sethu P. Cardiac Cell Culture Model As a Left Ventricle Mimic for Cardiac Tissue Generation. Anal Chem. 2013
39. Kensah G, Gruh I, Viering J, Schumann H, Dahlmann J, Meyer H, Skvorc D, Bar A, Akhyari P, Heisterkamp A, Haverich A, Martin U. A novel miniaturized multimodal bioreactor for continuous in situ assessment of bioartificial cardiac tissue during stimulation and maturation. Tissue Eng Part C Methods. 2011; 17:463–473. [PubMed: 21142417]
40. Wang B, Wang G, To F, Butler JR, Claude A, McLaughlin RM, Williams LN, deJonghCurry AL, Liao J. Myocardial scaffold-based cardiac tissue engineering: application of coordinated mechanical and electrical stimulations. Langmuir. 2013; 29:11109–11117. [PubMed: 23923967]
41. Morgan KY, Black LD 3rd. Mimicking Isovolumic Contraction with Combined Electromechanical Stimulation Improves the Development of Engineered Cardiac Constructs. Tissue engineering. Part A. 2014
42. Feng ZG, Matsumoto T, Nomura Y, Nakamura T. An electro-tensile bioreactor for 3-D culturing of cardiomyocytes - A bioreactor system that simulates the myocordium's electrical and mechanical response in vivo. Ieee Eng Med Biol. 2005; 24:73–79.
43. Chiu LL, Iyer RK, King JP, Radisic M. Biphasic electrical field stimulation aids in tissue engineering of multicell-type cardiac organoids. Tissue Eng Part A. 2011; 17:1465–1477. [PubMed: 18783322]
44. Iyer RK, Odedra D, Chiu LL, Vunjak-Novakovic G, Radisic M. Vascular endothelial growth factor secretion by nonmyocytes modulates Connexin-43 levels in cardiac organoids. Tissue engineering. Part A. 2012; 18:1771–1783. [PubMed: 22519405]
45. Zhang D, Shadrin IY, Lam J, Xian HQ, Snodgrass HR, Bursac N. Tissue-engineered cardiac patch for advanced functional maturation of human ESC-derived cardiomyocytes. Biomaterials. 2013; 34:5813–5820. [PubMed: 23642535]
46. Naito H, Melnychenko I, Didie M, Schneiderbanger K, Schubert P, Rosenkranz S, Eschenhagen T, Zimmermann WH. Optimizing engineered heart tissue for therapeutic applications as surrogate heart muscle. Circulation. 2006; 114:I72–178. [PubMed: 16820649]
47. Lim CC, Apstein CS, Colucci WS, Liao R. Impaired cell shortening and relengthening with increased pacing frequency are intrinsic to the senescent mouse cardiomyocyte. J Mol Cell Cardiol. 2000; 32:2075–2082. [PubMed: 11040110]

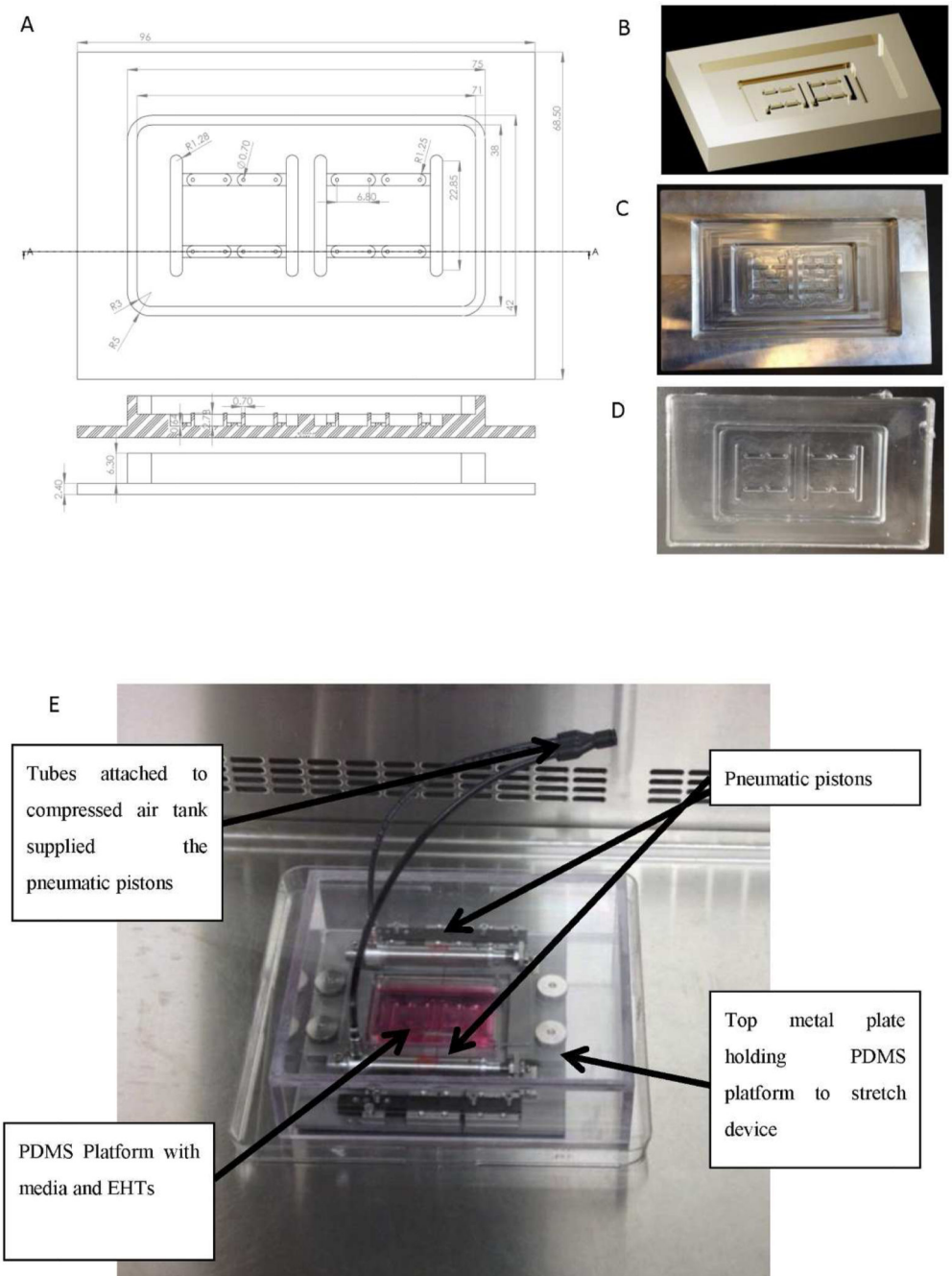

Figure 2. Bioreactor platform for combined electrical field and static stretch stimulation

A) CAD drawing of a bioreactor well capable of housing four cardiac microtissues and two pairs of stimulating electrodes. Each cardiac tissue microwell contains a par of posts to be used for monitoring of tissue contractions. B) Three-dimensional CAD rendering of the bioreactor well used in the milling machine for production of aluminum mold. C) Aluminum mold produced by the milling process. D) PDMS bioreactor wells produced using aluminum mold. E) PDMS bioreactor well placed in the pneumatically driven stretch device capable of providing static stretch.

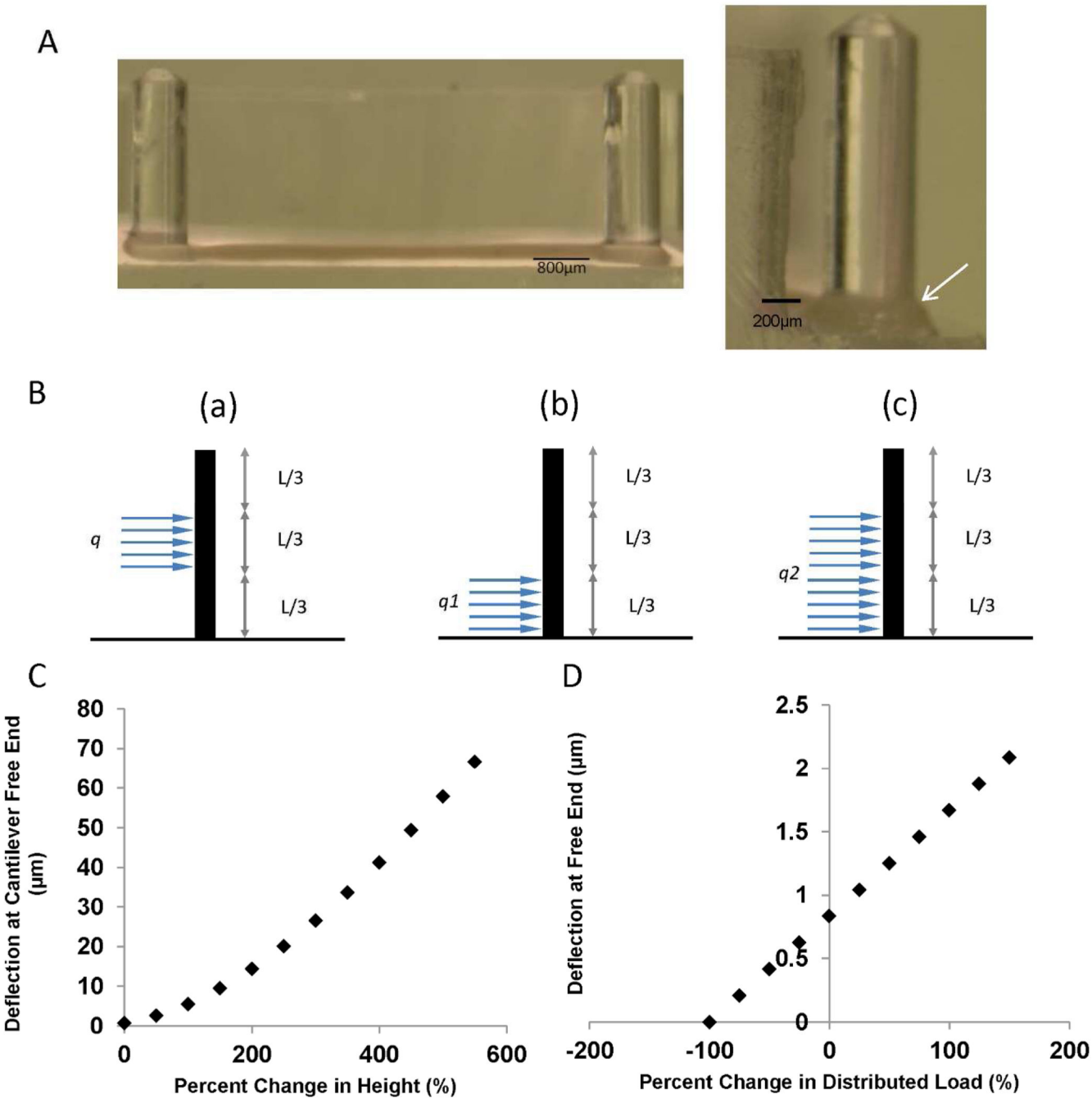

Figure 2. Validation of the strains and force of contraction measurements in the PDMS well of the bioreactor platform

A) Each cardiac tissue microwell contains a pair of posts that deflects as the tissue contracts. The tissue is generated by gel compaction of cardiomyocytes in a collagen gel (arrow). B) To calculate force of contraction, a beam deflection analytical model can be used to correlate imaged deflection of the post during a contraction cycle to force of contraction. If the tissue is not situated at the bottom of the post, a methods of superposition can be implemented to determine the distributed load on the post, where centrally positioned load (a) is modelled as a combination of two loads (b) and (c). The images are redrawn based on

a schematic presented in reference [20] C) Sensitivity analysis of post free end deflection with varying tissue height along the post. A tissue of 0.4 mm thickness situated at the bottom of the post with an average point force of contraction of 0.2 mN was the base scenario (0% height change) in this graph. The tissue was then moved up the post and the deflection at the free end was calculated again based on the same force of contraction. D) Sensitivity analysis of post free end deflection with varying distributed load. A tissue of 0.4 mm thickness situated at the bottom of the post with an average point force of contraction of 0.2 mN (0.5 N/m) was the base scenario at 0% change in distributed load. The distributed load was then varied while assuming the tissue remained at the bottom of the post.

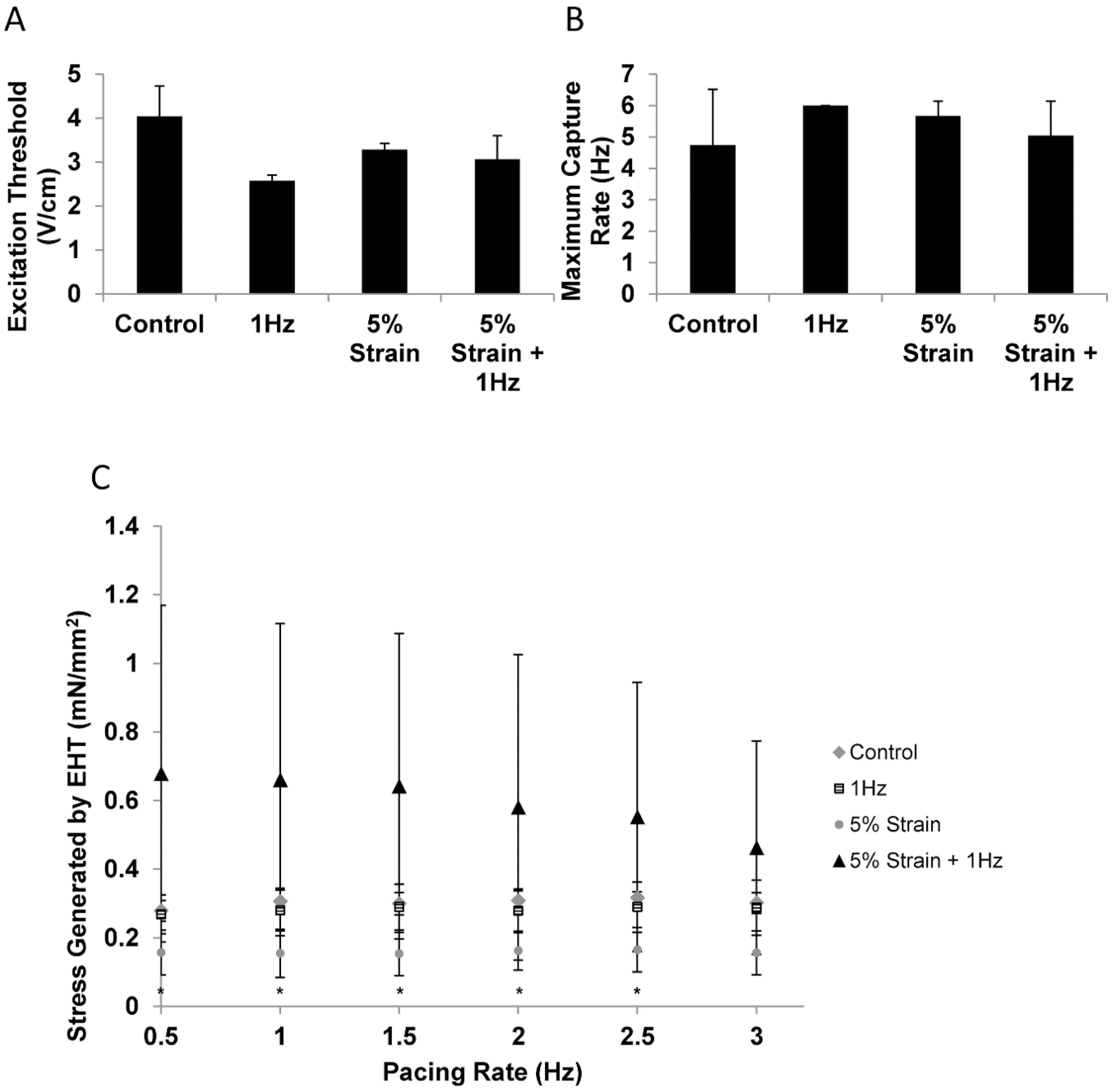

Figure 3. Functional properties of cardiac microtissues

A) Excitation threshold determined at the end of cultivation as a minimum voltage required to induce synchronous contraction. B) Maximum capture rate determined at the end of cultivation as the maximum tissue beating frequency. C) Force of contraction. Control- cardiac microtissues cultivated in the PDMS wells without electrical or mechanical stimulation. 1Hz- cardiac microtissues cultivated in the PDMS wells in the presence of electrical field stimulation at 1Hz. 5%- cardiac mictotissues cultivated in the PDMS stretched at 5% static strain without electrical stimulation. 5% strain + 1Hz- cardiac microtissues stretched at 5% static strain and concurrently subjected to electrical field

stimulation at 1Hz. * denotes statistical significant by Two-way ANOVA between 5% and 5% + 1Hz groups at specific pacing frequencies. Data represented as average ± standard deviation, N=3.

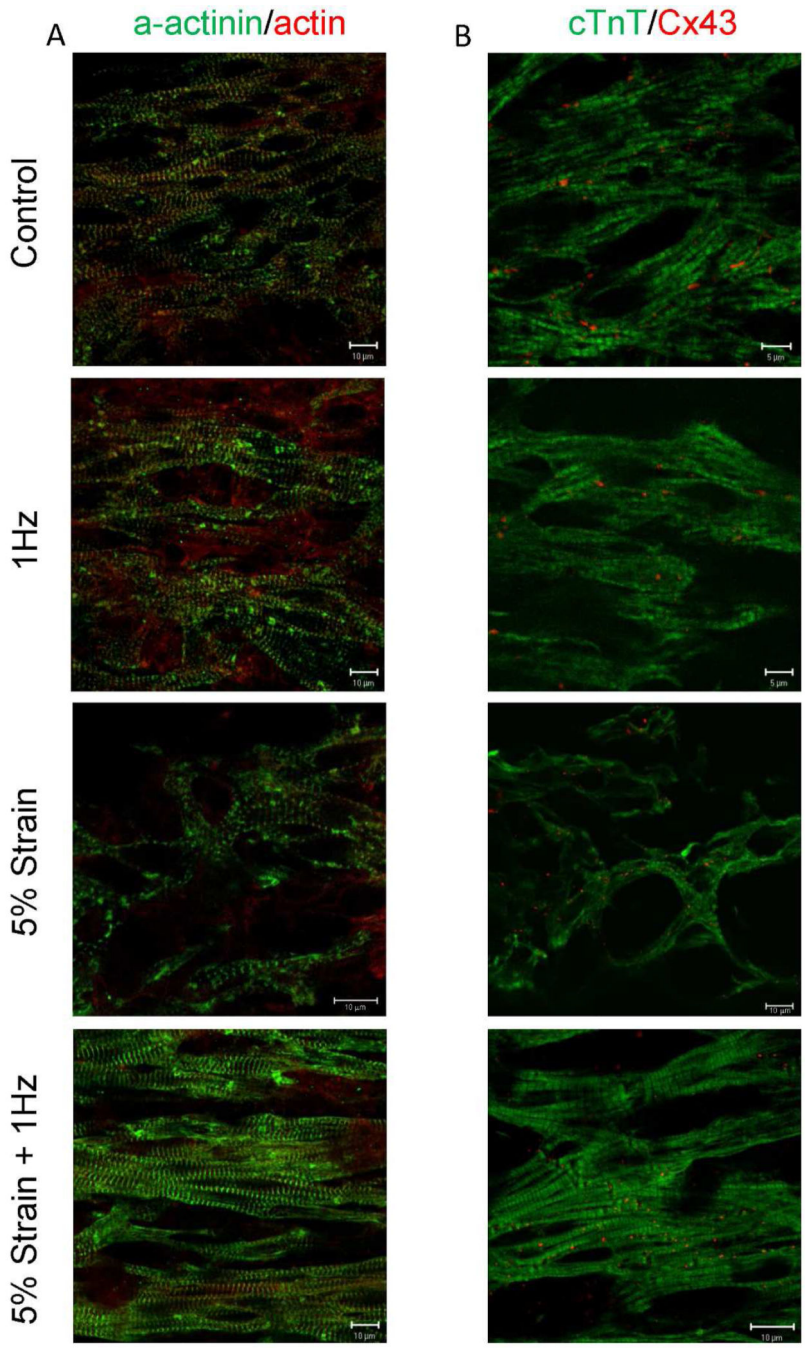

Figure 4. Immunostaining of cardiac microtissues for sarcomeric and gap junctional proteins

A) Double staining for sarcomeric α-actinin (green) and actin red. B) Double staining for cardiac troponin T (green) and connexion-43 red. Control-cardiac microtissues cultivated in the PDMS wells without electrical or mechanical stimulation. 1Hz- cardiac microtissues cultivated in the PDMS wells in the presence of electrical field stimulation at 1Hz. 5% strain + 1Hz- cardiac microtissues stretched at 5% static strain and concurrently subjected to electrical field stimulation at 1Hz.

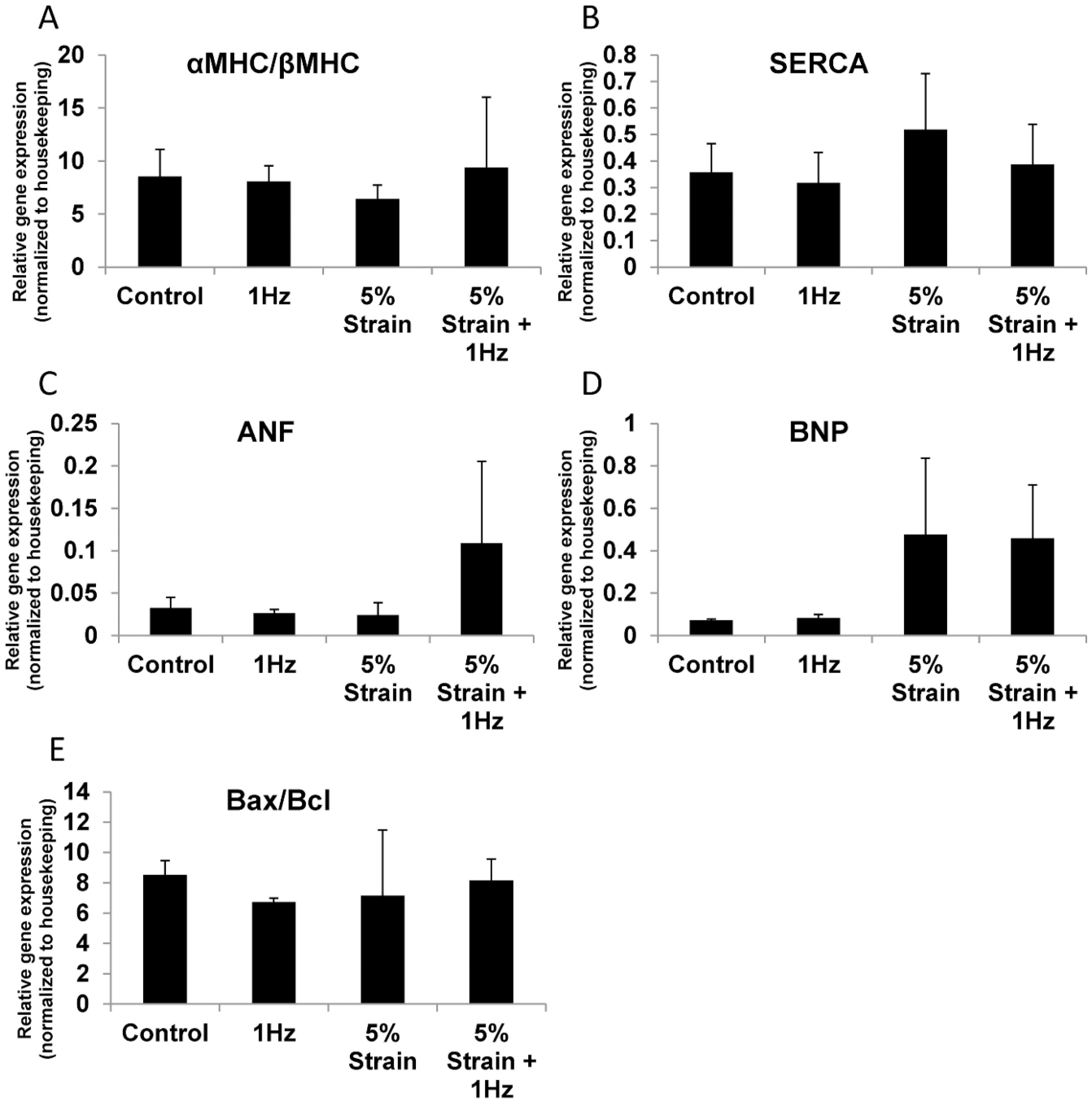

Figure 5. Quantitative polymerase chain reaction analysis cardiac genes in cardiac microtissues

A) Ratio of α-myosin heavy chain (MHC) to β-myosin heavy chain, B) Sarco/endoplasmic reticulum Ca^{2+}ATP-ase (SERCA), C) Atrial natriuretic factor (ANF), D) Brain natriuretic peptide (BNP), E) Ratio of pro-apoptotic Bax to anti-apoptotic Bcl-2. Data represented as averages ± standard deviation, N=3.

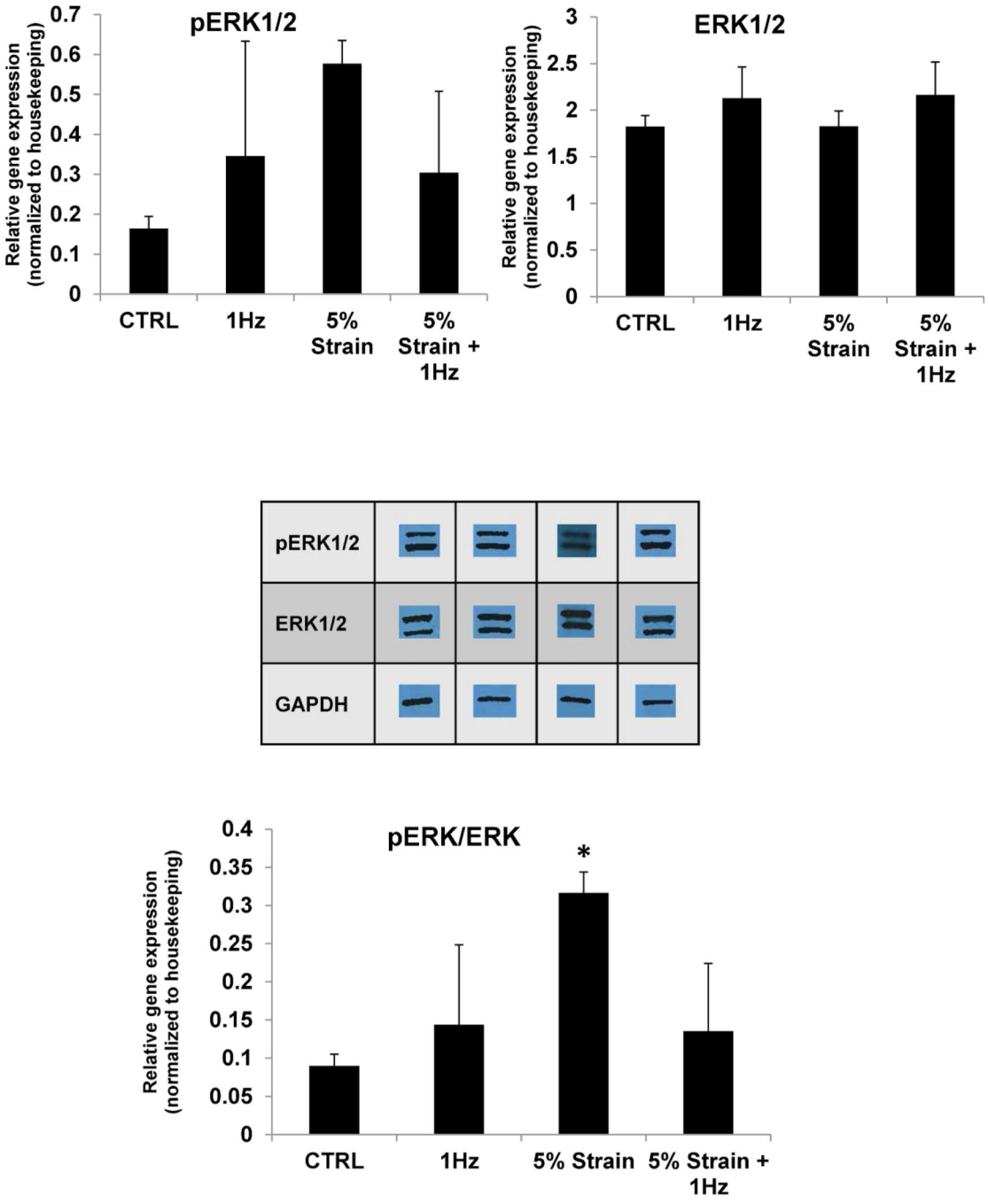

Figure 6. Western blotting for extracellular signal regulated kinases (ERK)1/2 expression and phosphorylation

* denotes statistical significance (P=0.032) between 5% strain and control group using One-way ANOVA. Data represented as averages ± standard deviation, N=3.

Table 1

Definition of variables used in post-deflection me asurements and force calculation

Symbol	Description	Units
q	Force per length	$\frac{N}{m}$
a	Distance of uniform load	m
E	Elastic Modulus	$\frac{N}{m^2}$
I	Area of moments of inertia ($\text{circle}=\frac{\pi r^4}{4}$)	m^4
L	Length of post	m
δ	Maximum deflection at free end of beam	m
FPA	Force per area	$\frac{N}{m^2}$
r	Radius	m

Table 2

Validation of the relationship between the measured strain in cardiac microtissue wells (i.e. distance between posts) and strain applied to the entire PDMS well

The PDMS well was stretched using the constructed stretching bioreactor. Images were taken of the PDMS platform at each of the four strain settings of 5, 10, 15 and 20%. The actual distance between the posts was measured and percentage error between the desired stretch and the average actual stretch was calculated as follows:

$$Percent\ Error = \frac{|Measured\ Strain - Applied\ Strain|}{|Applied\ Strain|} * 100$$

Average Measured Strain (%)	Applied strain (%)	Percent Error (%)
4.7 ± 0.1	5	9.8 ± 2.9
10.5 ± 0.9	10	7.7 ± 4.1
13.3 ± 0.2	15	12.5 ± 2.0
16.9 ± 0.6	20	18.4 ± 4.4

Table 3

Comparison between direct measurements of the force required to deflect a PDMS post and calculations based on the beam deflection model

The final column shows the percent error between the two methods calculated as follows:

$$Percent\ Error = \frac{|Measured\ Force - Calcualted\ Force|}{|Calculated\ Force|} * 100$$

Displacement is the distance the tip of a PDMS post was moved and the myograph force is the corresponding force recorded from the device required to move the PDMS post.

Displacement (μm)	Myograph Force (mN)	Analytical Solution Force (mN)	Percent error (%)
0	0.00	0.00	0.0
84	0.24	0.26	9.5
98	0.31	0.31	1.3
112	0.35	0.35	0.9
179	0.63	0.56	12.1
206	0.71	0.65	8.7
238	0.82	0.75	9.9